Volume 24 (1) 2025

Page 45 - 60

Mekanika: Majalah Ilmiah Mekanika

Mechanical Design and Prototype of Meatball Dough Grinder and Mixer Machine for Meat Processing in Indonesian Regions

Dandun Mahesa Prabowoputra[1*], Adi Febrianto Setiawan[2], Enrico Chandra Ramadhana[2], Welsa Okta Onistia[2], Robi Sulaiman[3], Rokhmat Arifianto[4], Gagah Hari Prasetyo[4]

1 Department of Mechanical Engineering, Universitas Jenderal Soedirman, Purbalingga, Indonesia
2 Department of Research and Development, P.T. Dimonitor Indonesia Sejahtera, Surakarta, Indonesia
3 Research Center for Process and Manufacturing Technology, National Research and Innovation Agency – BRIN, Tangerang Selatan, Indonesia
4 Directorate of Laboratory Management, Research Facilities, and Science and Technology Areas, National Research and Innovation Agency – BRIN, Jakarta Pusat, Indonesia

[*] Corresponding Author's email address: dandun.mahesa@unsoed.ac.id

Keywords:
Meatball dough
Grinding-mixing
Machine components
Design-prototype
Mechanical calculation

Abstract
A Meatball Dough Grinding-Mixing (MDGM) machine is a device that transforms raw meat into meatball dough through a combination of grinding and mixing processes, similar to a food processor or blender. The MDGM machine features four sharp stainless-steel blades. The rotation of the blade is driven by an electric motor with a power rating of 1 HP, operating at an engine speed of 2800 rpm. This engine speed is then transmitted through a belt pulley transmission with a diameter ratio of 3:5. The belt moves the installed blade at a rate of 1600 rpm. This MDGM machine has a capacity of 6 kg in one process. In this MDGM machine, one shaft stands vertically. The shaft has a diameter of 15 mm and a length of 400 mm. Pegs on the shaft, with dimensions of 6 mm in height and 6 mm in width, hold the rotating pulley in place when the engine is operating.

1 Introduction

Indonesian traditional meatballs known as *bakso* are produced from a mixture of finely ground meat with cooking salt, tapioca starch, and garlic. This batter is formed into balls ranging in size from a marble to a ping-pong ball and then cooked in boiling water. It is served with other stuff such as noodles, steamed/deep-fried tofu filled with minced meat, or steamed/deep-fried chow mien (a Chinese mixed spicy flour and minced meat in a thin dough sheet) or *bakso* itself in chicken/beef stock/soup. Peddlers typically distribute this product from pushcarts or small outlets along pedestrian walkways, at corners, or in restaurants [1-3]. Meatballs are processed food products [4]. They are liked by consumers of all age ranges, from the older to the younger generation [5]. Meatballs also have a high market which also supported by data that the consumption of *bakso* in Indonesia reached 2.5 kg per capita per year [6].

https://dx.doi.org/10.20961/mekanika.v24i1.97476

Revised 20 March 2025; received in revised version 24 March 2025; Accepted 29 March 2025
Available Online 31 March 2025

2579-3144

Corresponding to pioneer researcher's [7] statement, the quality of meatballs is highly affected by its composing ingredients, such as the quality of the meat. Meat with high-fat content will produce a coarse meatball texture [8]. Meatballs are processed comminuted meat, which can be classified as restructured meat, and are trendy in certain countries within the Asian region and some European countries. These products include Polpette from Italy, Koningsberger Klopse or meatballs in lemon and carper from Germany, Swedish meatballs from Swedia, Koefte from Turkey, Nunh Hoa from Vietnam, Curried Kofter from India, and Chinese meatballs of China [9-12] Asian meatballs are commonly produced by emulsifying delicate ground meat with starch, mixing salt and certain herbs specific to the ethnic cuisine, and shaping it into balls. Depending on the cuisine, they are then cooked in boiling water, steamed, or deep-fried. Like any other food, these products also contain elements (fat, cholesterol, salt, nitrite, phosphate, residues from environmental pollution or the use of pharmaceuticals, contaminants from disinfectants or detergents, toxic compounds formed during cooking, etc.) that, in certain circumstances and inappropriate proportions, harm human health [13]. The Indonesian National Standard [14] for *bakso* states that the product must have a moisture content of approximately 70%, a fat content of a maximum of 2%, protein content of a minimum of 6%, and an ash content of a maximum of 3%, and no borax must be detected [15]

Along with the development of the business and the increase in meatball production, small-scale meatball entrepreneurs face obstacles because they lack the necessary tools or machines to grind and knead the meatball dough. The Meatball Dough Grinding-Mixing (MDGM) machine will produce more dough much faster. Therefore, the MDGM machine is essential in grinding meat and kneading dough on a large scale. Based on this, the MDGM machine is designed and manufactured with a capacity of 8 kg for each process, utilizing an electric motor with a power of 1 HP. This design aligns with the philosophy of ease of use and low cost, enabling small-scale food industries to use it conveniently. The MDGM machine is considered better for making meatball dough because it can perform two processes simultaneously. Several components make up an electric motor, including a driving force, a shaft, a stirring knife, a mixing container, pulleys and belts for transmission, and a frame for mechanical support.

2 Literature Review

2.1 The Concept of Designing a Chopping Blade System in the MDGM Machine

The MDGM machine is designed for grinding and mixing meat, particularly for making meatball dough. Mincing and mixing raw meat and other materials is a crucial stage in manufacturing finely comminute meat products; it influences the properties of meat systems [16,17]. This machine aims to simplify the production of meatballs for meatball entrepreneurs. The bowl cutter can be used for industrial mincing and mixing of meat and other materials, maximizing the stability of the product [18], which relies on a rotating bowl with a series of rotating sharp knives. The beating machine disrupts connective tissues and myofibrillar structures with blunt blades (200 rpm) using a variable-speed crushing force, thereby enhancing friction forces and the exchange of soluble components in processed meats. Milling, in this context, refers to the process of cutting or chopping meat. Manual milling is performed by cutting meat using a knife that is moved directly by hand. Researchers in [19,20] reported that, compared to chopping, the Kung-Wans and frankfurters produced by beating had a better texture and higher cooking yield. However, few studies have reported the effects on physicochemical and rheological properties of meat batters made by chopping or beating [21]. This method results in fewer fine cuts of meat. Therefore, people, especially entrepreneurs and small business owners, need tools to help them.

The construction system should have a planning concept. The concept outlines the theoretical foundations that will serve as guidelines for the design. When designing the chopping knife system for the MDGM machine, specific components will be planned or calculated, including the power required to crush the meat and the cutting force necessary for the knife to cut it.

2.1.1 Meat Cut Force

Cutting force is the force required by the knife to cut the material. This force will later be used to determine the driving force of this machine and the power distributor for the shaft and other supporting components. In this design, the cutting force can be determined by knowing the material's shear stress and the area of the chopping area perpendicular to the blade (see Equation 1).

$$F = \tau_g \cdot A \tag{1}$$

The result of the cutting force is used to determine the total force, which is calculated based on the number of rotor blades (see Equation 2).

$$\sum F = F \cdot n_P \tag{2}$$

2.1.2 Chopping Blade Planning

Before determining the engine's driving power, it is necessary to know the rotation and torque used in the design. The rotation on the blade of this MDGM machine can be found in Equation 3.

$$n = \frac{v_C \cdot 1000}{\pi \cdot D} \tag{3}$$

Feeding speed can use the following Equation 4.

$$s_z = \frac{s}{z \cdot n} \tag{4}$$

The cutting capacity can be found using Equation 5.

$$Q = \rho \cdot v \tag{5}$$

Determining the weight of the knife can be performed using Equation 6.

$$Wn = L \cdot l \cdot t \cdot y \tag{6}$$

The tangential force of the blade can be found in Equation 7.

$$F_t = \frac{w_n}{g} \cdot \omega^2 \cdot r = \frac{w_n}{g}\left(\frac{2 \cdot \pi \cdot n}{60}\right)^2 \cdot r \tag{7}$$

Cutting power can be found using the following Equation 8.

$$N = \frac{F \cdot v}{75} \tag{8}$$

2.2 The Concept of Designing a Pulley and Belt System in the MDGM Machine

The MDGM machine enables small and Medium Sized Enterprises (SMEs) in the meatball manufacturing industry to produce meatballs more efficiently. This tool is designed to perform two processes: milling and stirring. In planning the construction system, a transmission system consisting of a belt and pulley is utilized. The quality of the pulleys significantly impacts the coupling timing belt with the pulley (see Figure 1). The pulley is connected with precision in terms of movement and displacement [22]. The V-belt drive system is typically designed for the specific function and operating conditions of the machinery [23]. It transmits power in many engineering applications, from a driver to a driven pulley. The V-belt drive consists of a V-belt mounted on two grooved pulleys, which are kept at a specified distance apart. The pulley groove angle is smaller than the belt section angle, allowing the belt to wedge into the groove and thereby increase friction. The side compression of the pulley walls yields elastic penetration into the groove, resulting in radial components of the friction forces [24-26]. The groove angle depends upon the belt section, pulley radius, and the contact angle of the belt and pulley. Because of this, an optimum groove angle is required for the system to avoid excessive belt pull on the pulley-shaft elements, which can result in unwanted vibration [27].

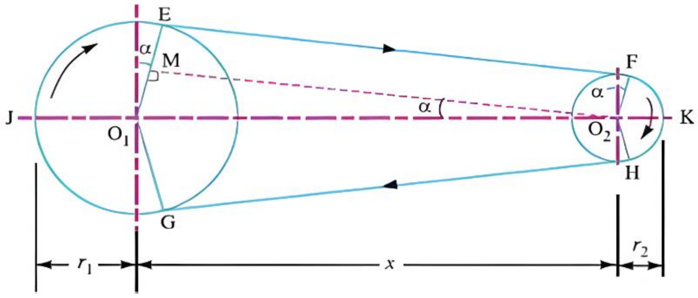

Figure 1. Tension in belt and pulley

The planning concept outlines the theoretical foundations that will serve as guidelines for the design. Reducing belt-pulley coupling is a primary concern during the design stage. Undesirable transverse span vibrations reduce belt life, produce noise, and accelerate fatigue. Significant belt vibrations can even cause the belt to jump a pulley groove, dramatically increasing belt stress that ultimately snaps the belt and fails the system [28].

A deeper understanding of these coupling mechanisms can enhance our knowledge of this system and provide valuable insights to designers of serpentine systems. Correspondingly, developing a mathematical model that captures the belt-pulley coupling is a primary objective of this research. This dynamic model should explain the large belt transverse vibration that occurs at the engine firing frequency, as observed by our research sponsor. Further analytical investigation of the design parameters of this belt-pulley coupling mechanism follows naturally. In planning the transmission system, several key factors will be considered, including determining engine power, pulley diameter, belt type, torque, belt length, belt contact angle, and selecting the correct belt.

2.2.1 Belt Calculation

1. Determining belt length (L)

The length of the circumference of the belt can be calculated by the following Equation 9.

$$L = \pi(r_1 + r_2) + 2x + \left(\frac{(r_1+r_2)^2}{x}\right) \tag{9}$$

2. The contact angle for an open belt

The surfaces of the belt and pulley grooves that touch form an angle that can be calculated by the following Equations 10 and 11.

$$sin\, a = \frac{r_1+r_2}{c} \tag{10}$$

$$\theta = (180 - 2 \propto)\frac{\pi}{180} \tag{11}$$

3. The tight side pull (T_1) and the slack side pull (T_2) on the belt

Figure 2 and Equation 12 illustrate the tension schemes for the vertical centrifugal casting machine's tight and loose sides.

$$2{,}31\, log\frac{T_1}{T_2} = \mu \cdot \theta \cdot cosec\, \beta \tag{12}$$

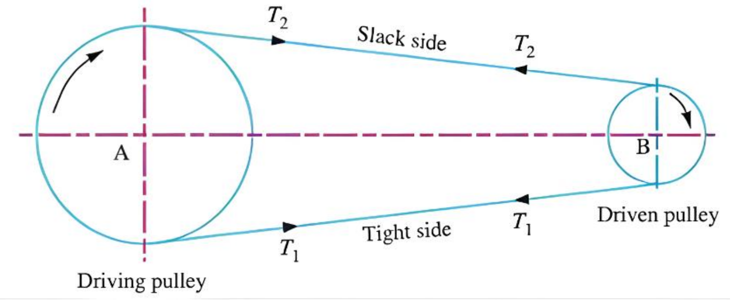

Figure 2. Pull the tight side (T_1) and the loose side (T_2)

4. Belt speed (v)

The belt rotates in conjunction with the rotating pulley, allowing for calculation of its linear speed using Equation 13. The belt specification is referenced in Tables 1 and 2.

$$v = \frac{\pi \cdot DP.n}{60} \tag{13}$$

Table 1. Specification and dimensions of the v-belt (1)

Type of belt	Power ranges in kW	Minimum pitch diameter of pulley (*D*) mm	Top width (*b*) mm	Thickness (*t*) mm	Weight per meter length in Newton
A	0.7 – 3.5	75	13	8	1.06
B	2 – 15	125	17	11	1.89
C	7.5 - 75	200	22	14	3.43
D	20 – 150	355	32	19	5.96
E	30 - 350	500	38	23	-

Table 2. Specification and dimensions of the v-belt (2)

Type of belt	w	d	a	c	f	e	No. of sheave grooves (n)	Groove angle (2β) in degrees
A	11	12	3.3	8.7	10	15	6	32, 34, 38
B	14	15	4.2	10.8	12.5	19	9	32, 34, 38
C	19	20	5.7	14.3	17	25.5	14	34, 36, 38
D	27	28	8.1	19.9	24	37	14	34, 36, 38
E	32	33	9.6	23.4	29	44.5	20	-

5. Belt surface size

The shape of the belt size is illustrated in Figure 2. The surface of the V-belt has a trapezoidal shape so that it can be calculated by the following Equations 14-16.

$$x = tan\beta \cdot t \tag{14}$$

$$c = b - 2x \tag{15}$$

$$A = \frac{1}{2}(b + C)t \tag{16}$$

6. Belt mass

The belt in the transmission system is made of a specific material or a combination of materials. Therefore, the mass of the belt can be calculated by following Equation 17.

$$m = A \cdot L \cdot \rho \tag{17}$$

7. Centrifugal tension on the belt (Tc)

When the pulley rotates, the belt generates tension in a circular direction, following the path of the pulley groove. This stress is called centrifugal tension, which can be calculated by Equation 18.

$$Tc = m \cdot v^2 \tag{18}$$

8. Maximum tensile tension of belt (T_{max})

The maximum tensile stress for the belt is the tensile stress, with the highest value acting on the belt when the pulley is in motion. The maximum tensile stress can be calculated in Equation 19.

$$T_{max} = \sigma_{max} \cdot A \tag{19}$$

9. Style on belt

Belts can be safe if the force on the belt does not exceed the maximum belt tension. The check force on the belt can be calculated by Equation 20.

$$T = T_1 - T_2 \tag{20}$$

10. Belt transmitted power (P_b)

The power transmitted by the belt is used to determine the maximum power that a single belt can transmit. This is important for determining the number of belts. The power transmitted by the belt can be calculated by the following Equation 21.

$$P_{b=(T_1-T_{2)}\cdot V} \tag{21}$$

11. Number of belts (n_b)

From the amount of power transmitted by the belt, the number of belts used will be searched using the following Equation 22.

$$n_b = \frac{P}{P_b} \tag{22}$$

2.2.2 Pulley

A pulley is a component used to run a flow force, which works to deliver power. The pulley works to change the direction of the applied force, send motion, and change the direction of rotation of the driven pulley diameter (see Equation 23).

$$d_2 = \frac{d1 \cdot N_1}{N_2} \tag{23}$$

2.3 Shaft and Stake Design Concepts in the MDGM Machine

The construction system should have a planning concept. The planning concept outlines the theoretical foundations that will serve as guidelines for the design. Configuration design is a design approach that provides a set of predefined components, which can be interfaced (connected) in predefined ways and then assemble the selected components. The term "component" is used in a generic sense to encompass special-purpose parts, standard parts, and standard assemblies [29]. In the design of shafts and pins, various components must be planned or calculated, including the power transmitted by the shaft, the force acting on the shaft, and the strength of the pin. A shaft is a rotating member, usually of a circular cross-section, used to transmit power or motion. It provides the axis of rotation or oscillation for elements such as gears, pulleys, flywheels, cranks, and sprockets and controls the geometry of their motion [30]. The shaft is the most vital component in almost every mechanical system and machine. Among all power transmission components, the shaft is the primary component that must be carefully designed for efficient machine operation. The discontinuities in the shaft are prime causes for shaft failure due to a reduction in shaft strength. The shaft design for combined loading is the most critical problem in practical applications. In most practical applications, the shaft must be designed for combined loadings. The shaft withstands a whole load of the machine. Therefore, the shaft design is essential to mechanical design [31]. Shafts are subjected to various loading conditions depending on their application. Various types of loading are considered while designing the shaft. Essential loading for the shaft is torsional, as it is always present in any shaft [32]. Therefore, it must be designed for shear stresses in any application. Pioneer researchers have designed the shaft of an inertia dynamometer, which is subjected to combined bending and torsion [33-35], based on calculations of force and torque. The following formulas are used to calculate the shaft (Equations 24-27).

a. Torque on the shaft

$$T = \frac{P \cdot 60}{2 \cdot \pi \cdot N} \tag{24}$$

b. The moment that occurs on the shaft

$$M = F.\,L \tag{25}$$

c. Torque equivalent

$$M = F.\,L \tag{26}$$

d. Shaft diameter

$$d = \sqrt{\frac{16 \cdot Te}{\pi \cdot \bar{\iota}_s}} \tag{27}$$

3 Methodology

3.1 Planning Stage

- Literature study. This process aims to collect as much information as possible in the field about the conditions that the product must meet in terms of specification requirements, as well as its advantages and disadvantages, components, and other relevant details. Next, the points of the problem that need to be solved are identified. From here, the technical specifications that must be met for the product will be obtained, allowing it to be implemented in actual field conditions.
- Sketch. This process begins with collecting data, a theoretical basis, and literature from relevant sources to serve as reference materials, as well as references for designing machines in the form of sketches, which facilitate easier problem-solving for designers. After that, they collected as many concept ideas as possible about the design of the MDGM machine. Sketching by hand before creating a machine design in the SolidWorks application is essential. After the sketch has been approved, a 3D model is developed using SolidWorks.
- Power and component calculations. Before proceeding to a more detailed process, the existing 3D design is evaluated, and each component is analyzed. Additionally, the machine's power and detail must be carefully calculated to prevent machine failure from causing it to malfunction later.
- Engineering drawings. After all sizes and designs are declared functional, detailed drawings and dimensions (2D and 3D Drawings) of the MDGM machine design are made. This simplifies the production process, from material procurement to assembly and archiving, ensuring a seamless manufacturing process.
- Production process planning aims to minimize the risk of errors during the production process, especially processes that must be carried out sequentially so that work takes place optimally and no material is wasted.
- Production and assembly. The next step is the component assembly process, which follows the purchase of all materials and the completion of the manufacturing process. Components are assembled in sequence according to the assembly process until the machine is fully assembled.

- Testing. The finished machine is then tested to determine if any parts require any repair before being used in the field. It is tested for its performance in grinding and mixing the meat to be *bakso*.
- The data obtained from the testing process is then used as the basis for the tool repair process. So that when the machine is used in actual conditions, it can work optimally without any problems. If components do not work as they should in testing, the next step is to make repairs, starting from the initial step.
- Compiling reports. After the machine has been manufactured and no further errors have been identified, the next step is to compile a report based on the existing systematics and instructions for use and care. The flowchart of the planning process is shown in Figure 3.

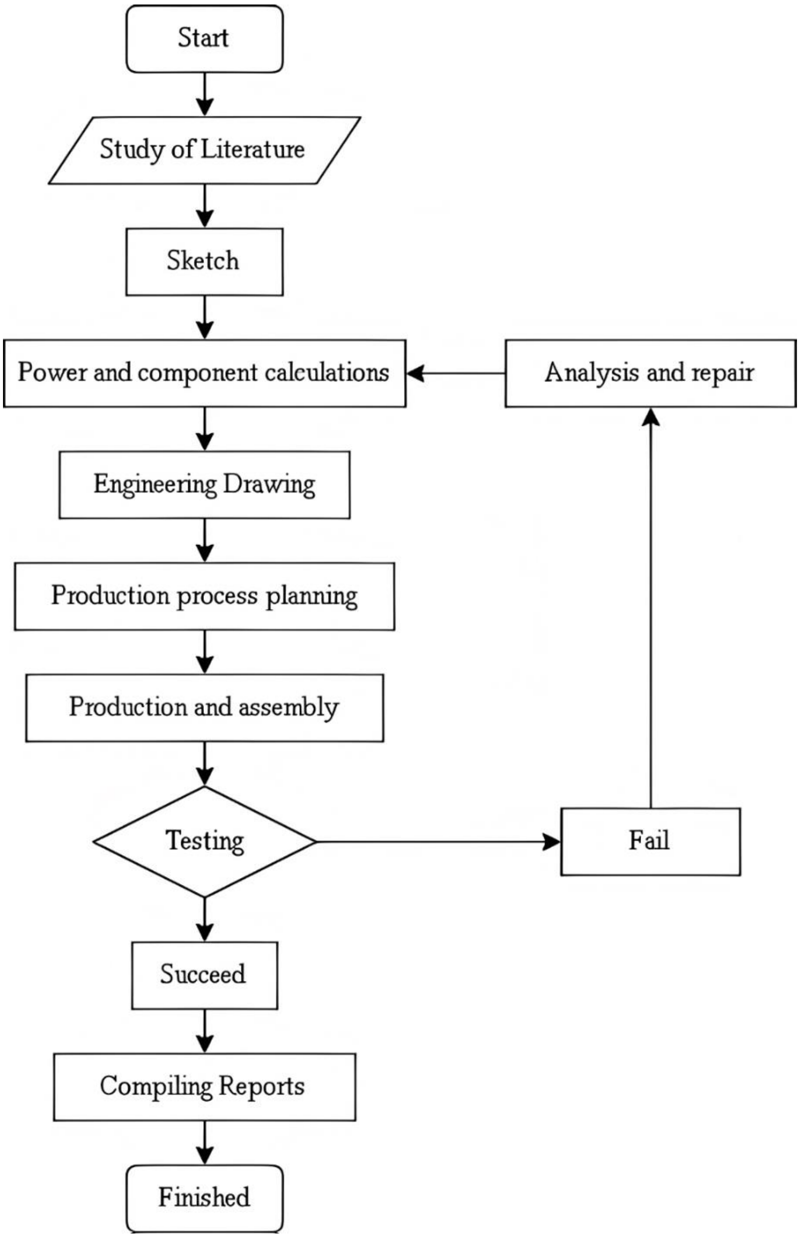

Figure 3. The MDGM machine planning flow chart

3.2 Product Identification

This MDGM machine made it easier for meatball entrepreneurs to produce meatball dough on a medium to low scale. With this MDGM machine, small and medium-scale meatball entrepreneurs can save time and costs that they previously incurred by grinding and kneading meatball dough in-house. Things to consider are:

1. Looking for the mechanism literature on how the Meatball Grinding and Mixing Machine can simultaneously work with two processing processes.
2. Looking for data about the chopping knife system as a component for grinding and mixing meatball dough.
3. Looking for data about the shaft as a power transmission from the electric motor to the cutting blade.
4. Looking for data about the transmission system as a successor to the rotation of the electric motor to the shaft.

3.3 Machine Drawing Model

Figure 4 shows the final project sketch planning, titled Meatball Dough Grinding-Mixing (MDGM) machine. Table 3 describes the image of the MDGM machine.

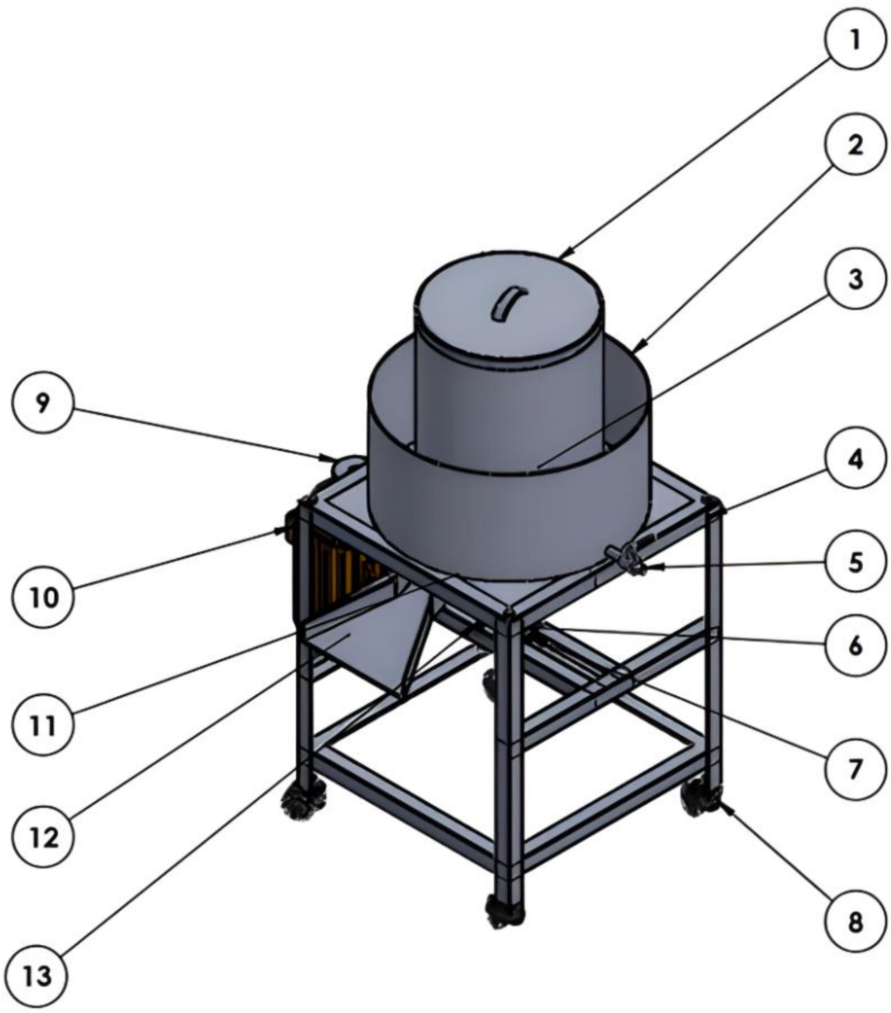

Figure 4. The MDGM machine drawing model

Table 3. Description of the meatball dough grinding-mixing machine

No.	Description	No.	Description
1	Close the top of the *dandang*	8	Wheel
2	*Dandang*	9	Pulley
3	Knife	10	Electric motor
4	Frame	11	Close the bottom of the *dandang*
5	Valve	12	Reservoir channel
6	Bearing	13	Shaft
7	V-Belt		

4 Results and Discussion

4.1 Meat Cut Force

Calculating the fundamental requirements of force performance required for a system to work is essential. In this work, it is assumed that the processed meat in a cycle process is 8 kg, and the force for this will be needed to calculate the transmission system and engine capacity. The summarized calculation using Equations 28-30 is presented in Table 4.

Table 4. The obtained technical details for the meat cut force

Variable	Formula	Equation no.	Results
Meat cut force to cut 8 kg of meat	$F = 254grf$	(28)	F = 4.98 N
Transmission system selection in the form of a driven pulley	$N_1 \cdot d_2 = N_2 \cdot d_1$	(29)	N_2 = 1680 rpm
Engine speed planning	$v = \frac{\pi \cdot DP \cdot N}{60}$	(30)	v = 24.61 m/s

4.2 Calculation of Transmission System (Pulley and V-belt)

The pulley is selected based on the summarized calculation using Equations 31 and 32 in Table 5. It can be seen that the primary considerations for the pulley are torque and motor power. Based on the obtained values, the planned pulley specification is given as follows:

- Rotating speed on motor = 2800 rpm
- Shaft axis distance = 343.57 mm
- Pulley 1 (d_1) = 76.2 mm
- Pulley 2 (d_2) = 127 mm

Table 5. The obtained technical details for the pulley

Variable	Formula	Equation no.	Results
Torque at T_1	$T_1 = \frac{T_2 \cdot N_2}{N_1}$	(31)	T_1 = 597.6 N/m
Motor power	$P = T \cdot \omega$	(32)	P = 0.87 HP ≈ 1 HP

The belt type can be calculated using the parameters of the electric motor power and the rotation of the small pulley and pulley driver. Based on the electric motor used, the small pulley rotates at 2800 rpm. The choice of belt type can be found using the diagram in [36], which can be concluded that the selected belt is a V-belt type A with the specification as follows:

- Material = rubber
- Wide (b) = 13 mm
- Thick (t) = 8 mm
- Pulley angle (2β) = 34°
- Belt density (p) = 1140 kg/m³
- Max. tensile stress (σ_{max}) = 2.1 MPa

Further calculations for the belt will be directed to several parameters, i.e., belt length (L), belt contact angle (α), belt speed (V), tight and slack side pull (T_1 and T_2), belt cross-sectional area (A), belt mass per meter (M), belt centrifugal force (T_C), belt maximum tension (T), belt transmitted power (p_b), and a total of the belt (η_b). The summarized calculation using Equations 33-42 is presented in Table 6, while the illustrations for length and cross-sectional area calculations are presented in Figures 5 and 6.

Table 6. The obtained technical details for the belt

Variable	Formula	Equation no.	Results
Belt length (L)	$L = \pi(r_1 + r_2) + 2x + (\frac{(r_{1-}r_2)2}{x})$	(33)	L = 1047.93 mm
Belt contact angle (α)	$\sin x = \frac{r_1 - r_2}{x_1}$	(34)	α = 3.03 rad
Belt speed (V)	$V = \frac{\pi \cdot D_2 \cdot N_2}{60}$	(35)	V = 5.58 m/s
Tight and slack side pull (T_1 and T_2)	$2.31 \log \frac{T_1}{T_2} = \mu \cdot \theta \cdot \operatorname{cosec} \beta$	(36)	$\frac{T_1}{T_2} = 22.13$
Belt cross-sectional area (A)	$\tan 17° = \frac{x}{t}$	(37)	A = 0.000084 m²
Belt mass per meter (M)	M = area x length x density	(38)	M = 0.100 kg/m
Belt centrifugal force (T_C)	$T_c = M \,.\, (v)^2$	(39)	T_C = 3.11 N
Belt maximum tension (T)	$T = \sigma \cdot a$	(40)	T = 7.87 N
Belt transmitted power (p_b)	$p_b = (T_1 - T_2)V$	(41)	p_b = 9.282 kW
Total of the belt (η_b)	$n_b = \frac{P}{p_b}$	(42)	$\eta_b = 0.36 \approx 1$

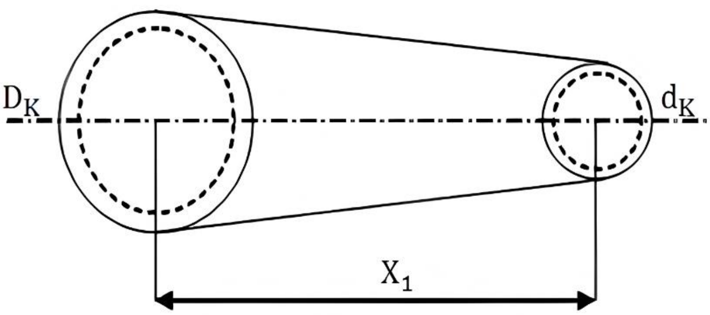

Figure 5. Description of the belt length calculation

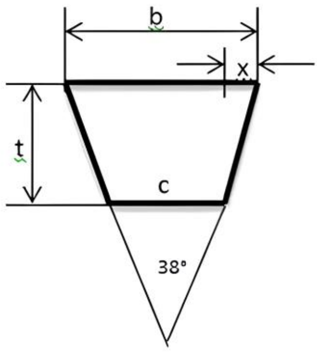

Figure 6. V-belt cross-section

4.3 Shaft Calculation

The shaft calculation can be calculated with the following data: the motor power (P) is 653.376 W, the rotation speed (N) is 1680 rpm, the shaft material used is ST37 steel, shear stress r (τ_s) of 170 N/mm^2, bending stress (σ_b) of 340 N/mm^2, pulley tension on the shaft is 182.07 N, pulley force on the shaft is 1.746 N and the force on the grinder and stirrer is 86.328 N. The calculation of the force on the cutting knife and grinder, as determined by Equations 43-48, is presented in Table 7. Then, the shaft force balance schematic is illustrated in Figure 7 and summarized in Table 8.

Table 7. Forces on cutting and grinding blades

Variable	Formula	Equation no.	Results
Shaft torque (T)	$T = \frac{60 \times P}{2\Pi N_2}$	(43)	T = 3.715 Nm
Style on cutting blades and grinders (F_{ps})	$F_{PS} = \frac{T}{R}$	(44)	F_{ps} = 26.53 N

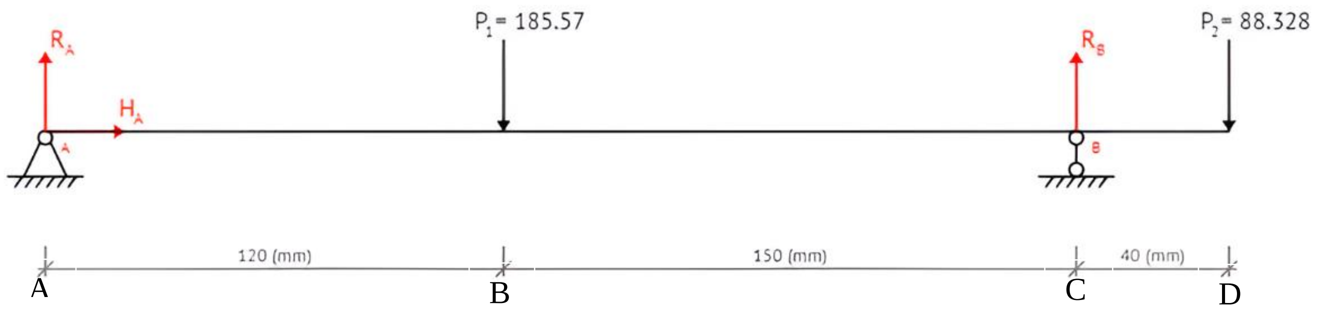

Figure 7. Schematic balance of shaft forces

$\sum M_A = 0$
R_{cy} = 183.8 Nmm (in the direction according to the red arrow)

$\sum F_y = 0$
R_{ay} = 90.009 N (in the direction according to the red arrow)

Table 8. Calculation of the moment on the shaft. Graphical illustration is displayed in Figures 8 and 9.

Variable	Formula	Equation no.	Results
Moment at point A (M_A)	$M_A = 90.009\ \mathrm{N}\ .\ x$	(45)	$M_A = 0$
Moment at point B (M_B)	$M_B = 90.009\ \mathrm{N}\ .\ x$	(46)	M_B = 10,801.08 Nmm
Moment at point C (M_C)	$M_C = 90.009\ \mathrm{N}\ (120 + x) - R_{by}\ .\ x$	(47)	M_C = - 3,533.07 Nmm
Moment at point D (M_D)	$M_D = 90.009\ \mathrm{N}\ (270 + x) + R_{by}\ (150 + x) + R_{cy}.\ x$	(48)	$M_D = 0$

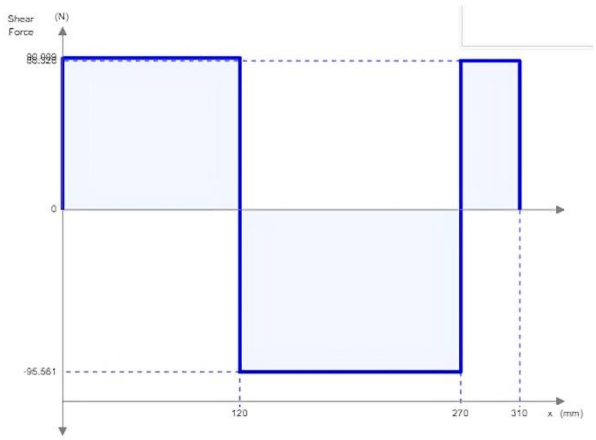

Figure 8. Shear force diagram (SFD)

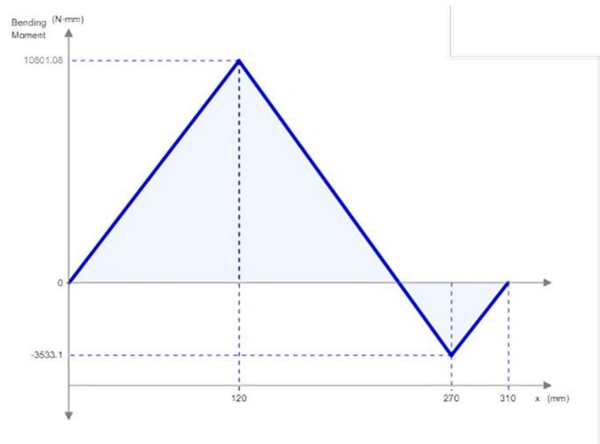

Figure 9. Bending moment diagram (BMD)

The shaft diameter (see Table 9) is selected based on an equivalent torque of at least 8 mm and an equivalent moment of at least 8.56 mm (the calculation is conducted using Equations 49-52). Therefore, the shaft is safe and can be adapted to available bearings. Finally, the used shaft has a diameter of 15 mm.

Table 9. Calculation of shaft diameter (d)

Variable	Formula	Equation no.	Results
Torque equivalent (T_e)	$Te = \sqrt{(k \times m)^2 + (kt \times T)^2}$	(49)	T_e = 17,133.16 Nmm
Shaft diameter (d)	$d = \sqrt[3]{\frac{16 \times Te}{\Pi \times \tau_s}}$	(50)	d = 8 mm
Equivalent moment (M_e)	$Me = \frac{1}{2}[km\, x\, (M + \mathrm{Te})]$	(51)	M_e = 20950.68 N
Shaft diameter (d)	$d = \sqrt[3]{\frac{32xMe}{\Pi x \sigma_b}}$	(52)	d = 8.56 mm

4.4 Counting Knife Calculation

The planning of the chopping knife to be used is related to the desired blade rotation and whether it can cut meat with a capacity of 6 kg. The knife's design is illustrated in Figure 10. The summarized calculation, using Equations 53-57, for the knife design is presented in Table 10.

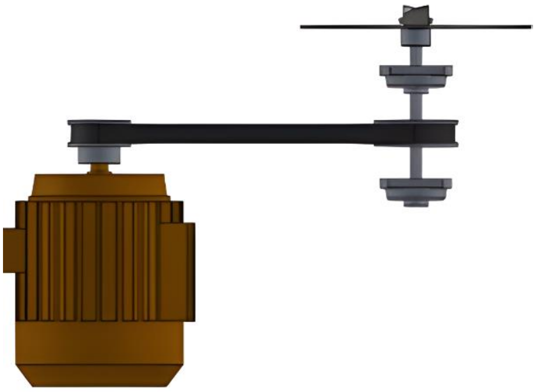

Figure 10. Illustration of chopping knife planning

Table 10. Calculation of the knife design

Variable	Formula	Equation no.	Results
Cutting rotation speed (v_{rot})	$v_{rot} = \frac{\pi \cdot D \cdot n}{1000 \cdot 60}$	(53)	v_{rot} = 0.5 m/s
Cutting result speed (v_{res})	$v_{res} = \frac{\pi \cdot D \cdot n}{1000}$	(54)	v_{res} = 0.03 m/min
Cutting capacity (Q)	$Q = \rho \cdot v$	(55)	Q = 26.43 kg/h
Blade weight (W_n)	$Wn = L \cdot l \cdot t \cdot y$	(56)	W_n = 0.19 kg
Tangential force (F_t)	$F_t = \frac{w_n}{g}\left(\frac{2 \cdot \pi \cdot n}{60}\right)^2 \cdot r$	(57)	F_t = 408.7 N

4.5 Machine Design Result and Testing

Tests are conducted to evaluate the machine's performance by feeding it 1 kg of beef and the dough ingredients. The grinding time and smoothness of the meatball dough are considered in this test. It takes approximately three minutes to make a smooth meatball dough and the seasonings. The results of the design of the Meatball Dough Grinding-Mixing (MDGM) machine are shown in Figure 11. The obtained machine specifications are:

- The driving motor power is 1 HP (746 W)
- The shaft diameter is 15 mm, made of ST37 steel, with a 6 mm high and 6 mm wide keyway.
- Drive pulley diameter = 76.2 mm, driven pulley diameter = 127 mm.
- The pulley belt used is a V-belt no. = 39, L = 1047 mm.
- The bearings used in this machine have a diameter of 15 mm.

Figure 12 shows that the test results for 1 kg of beef, ground for 1 minute, were already smooth. Compared to existing machines on the market, this designed MDGM machine is more efficient because it takes approximately 5 minutes to produce the same results as those machines. Based on Figure 12, the results of grinding with seasoned meatballs are shown. The ingredients used are egg, wheat, tapioca flour, pepper, and meatball seasoning. To achieve the result presented in Figure 13, the designed MDGM machine takes 3 minutes to form a dough. Compared to existing machines on the market, this MDGM is still more efficient because it takes only 10 minutes to produce the same amount of dough using the same ingredients.

Figure 11. Meatball dough grinding-mixing machine: actual size

Figure 12. The results of the meat grinder

Figure 13. Results of ground beef and meatball seasoning

5 Conclusions

- The machine uses a 1 HP motor with a drive shaft diameter of 15 mm, a drive pulley diameter of 76.2 mm, and a pulley driver of 127 mm. The pulley belt used is a V-type belt no = 39 with L = 1047 mm.
- This machine is designed with a maximum capacity of 6 kg.
- The material used in the design of the shaft is ST37 steel, while the material used in the design of the chopping knife and dough container/pan in this MDGM machine is SS 304 series stainless steel and is included in the food-grade category.
- Lathes, hand grinding machines, and milling machines are used in the manufacture of this machine. The supporting equipment used is a right-aligned HSS chisel, inner chisel, center drill, rotary center, end mill cutter diameters of 10 mm and 25 mm, vise, caliper, and Occupational Health and Safety equipment (K3).
- It takes 3 minutes to conduct grinding and stirring the beef until it becomes a smooth meatball dough.

References

1. H. Rahmania, Sudjadi, and A. Rohman, “The employment of FTIR spectroscopy in combination with chemometrics for analysis of rat meat in meatball formulation,”. *Meat Sci.*, vol. 100, pp. 301-305, 2015.
2. S. F. Persada, R. D. Kumalasari, M. Shanti, K. Lukiyanto, G. S. Putri, C. A. Ramadhan, M. N. Young, and Y. T. Prasetyo, “How Social Media Reacting to Bakso Malang as Culinary Business on Post Covid 19: A Sentiment Analysis,” *Proc. Comput. Sci.*, vol. 234, pp. 463-469, 2024.
3. E. Kurniawati, A. Rohman, and K. Triyana, “Analysis of lard in meatball broth using Fourier transform infrared spectroscopy and chemometrics,” *Meat Sci.*, vol. 96, pp. 94-98, 2014.
4. D. D. Sinaga, Herpandi, and R. Nopianti, “Karakterisitik Bakso Ikan Patin (*Pangasius pangasius*) dengan Penambahan Karagenan, Isolat Protein Kedelai, dan Sodium Tripolyphospat,” *Jurnal Teknologi Hasil Perikanan*, vol. 6, no. 1, pp. 1-13, 2017. (*In Indonesian*).
5. A. Saputrayadi, Asmawati, Marianah, and Suwati, “Analisis Kandungan Boraks dan Formalin pada Beberapa Pedagang Bakso di Kota Mataram,” *Jurnal Agrotek Ummat*, vol. 5, no. 2, pp. 107-116, 2018. (*In Indonesian*).
6. S. M. Nasaruddin, S. P. Utama, and A. Andani, “Nilai Tambah Pengolahan Daging Sapi Menjadi Bakso pada Usaha Al-Hasanah di Kelurahan Rimbo Kedui Kecamatan Seluma Selatan.” *Agrisep*, vol. 14, no. 1, pp. 85-96, 2015. (*In Indonesian*).
7. A. Astati, “Tingkat Perubahan Kualitas Bakso Daging Sapi Bali Bagian Sandung Lamur (*Pectoralis profundus*) Selama Penyimpanan dengan Pemberian Asap Cair,” *Jurnal Teknosains*, vol. 7, no. 1, pp. 10-19, 2013. (*In Indonesian*).
8. M. C. Pamungkas, B. D. Probowati, and I. Maflahah, “Pengukuran Preferensi Konsumen Bakso,” *Agrointek*, vol. 8, no. 1, pp. 32-39, 2014. (*In Indonesian*).
9. M. Fulton, *Encyclopedia of Food and Cookery*, New York: Gallery Books, 1986.
10. B. Duong and M. Kiesel, *Simple Art of Vietnamese Cooking*, New Jersey: Prentice Hall Press, 1991
11. V. R. Redden and T. Chen, “The Potential Chinese Meatballs and Dried Meat as Value Added PSE Pork Product,” *Food Australia*, vol. 47, pp. 323-326, 1995.
12. M. Serdaroglu and O. Degirmencioglu, “Effects of Fat Level (5%, 0%, 20%) and Corn Flour (0%, 2%, 4%) on Some Properties of Turkish Type Meatballs (Koefte),” *Meat Sci.*, vol. 68, pp. 291-296, 2004.
13. F. Jimenez-Colmenero, J. Carballo, and S. Cofrades, “Healthier Meat and Meat Products: Their Role as Functional Foods,” *Meat Sci.*, vol. 59, pp. 5-13, 2001.
14. Badan Standardisasi Nasional, *SNI 01-3818-1995: Bakso Daging*, Jakarta: Badan Standardisasi Nasional, 1995. (*In Indonesian*).
15. E. S. Widyastuti, *Studi tentang Penggunaan Tapioka, Pati Kentang dan Pati Modifikasi dalam Pembuatan Bakso Daging Sapi (Study on the Incorporation of Tapioca Starch, Potato Starch and Modified Starches in the Production of Beef Bakso),* Malang: Brawijaya University, 1999.
16. B. D. Tobin, M. G. O’Sullivan, R. M. Hamill, and J. P. Kerry, “The Impact of Salt and Fat Level Variation on the Physio-Chemical Properties and Sensory Quality of Pork Breakfast Sausages,” *Meat Sci.*, vol. 93, pp. 145-152, 2013.
17. S. Banon, P. Diaz, G. Nieto, M. Castillo, and D. Alvarez, “Modelling the Yield and Texture of Comminuted Pork Products Using Color and Temperature. Effect of Fat/Lean Ratio and Starch,” *Meat Sci.*, vol. 80, pp. 649-655, 2008.

18. I. Allais, C. Viaud, A. Pierre, and E. Dufour, “A Rapid Method Based on Front-Face Fluorescence Spectroscopy for the Monitoring of the Texture of Meat Emulsions and Frankfurters,” *Meat Sci.*, vol. 67, pp. 219-229, 2004.
19. Z. L. Kang, Y. F. Zou, X. L. Xu, C. Z. Zhu, P. Wang, and G. H. Zhou, “Effect of Various Amount of Pork and Chicken Meat on Sensory and Physicochemical Properties of Chinese-Style Meatballs (Kung-wan).” *Food Sci. Technol. Res.*, vol. 19, pp. 963-970, 2013.
20. Z. L. Kang, Y. F. Zou, X. L. Xu, C. Z. Zhu, P. Wang, and G. H. Zhou, “Effect of a Beating Process, As a Means of Reducing Salt Content in Chinese-Style Meatballs (Kung-Wan): A Physico-Chemical and Textural Study.” *Meat Sci.*, vol. 96 pp. 147-152, 2014,.
21. Z. L. Kang, P. Wang, X. L. Xu, C. Z. Zhu, K. Li, and G. H. Zhou, “Effect of a Beating Process, As a Means of Reducing Salt Content in Frankfurter: A Physico-Chemical and Raman Spectroscopic Study.” *Meat Sci.*, vol. 98, pp. 171-177, 2014.
22. G. Domek, A. Kołodziej, M. Dudziak, and T. Woźniak, “Identification of the Quality of Timing Belt Pulleys,” *Proc. Eng.*, vol. 177, pp. 275-280, 2017.
23. P. P. Jombo and G. A. Adetona, “Computer-Aided Design of Belts and Pulley Systems,” *Nigerian J. Eng. Res. Dev.*, vol. 2, pp. 1-11, 2003.
24. F. Sorge, “A Qualitative-Quantitative Approach to V-Belt Mechanics,” *J. Mech. Des.*, vol. 118, pp. 15-21, 1996.
25. G. Gerbert, *Traction Belt Mechanics*, Göteborg: Chalmers University of Technology, 1999.
26. G. Gerbert and F. Sorge, “Full Sliding ‘Adhesive-Like’ Contact of V-Belts,” *J. Mech. Des.*, vol. 124, pp. 706-712, 2002.
27. N. A. Raji, A. A. Erameh, A. A. Yussouff, and R. O. Durojaye, “Response Surface Methodology Approach for Transmission Optimization of V-Belt Drive,” *Modern Mech. Eng.*, vol. 6, pp. 32-43, 2016.
28. L. Kong, *Coupled Belt-Pulley Mechanics in Serpentine Belt Drives*, Colombus: The Ohio State University, 2003.
29. R. H. A. Haq, M. F. Hassan, S. Mahmood, and M. H. A. Hamid. “Fish Ball Maker Machine for Household Chores,” *J. Des. Sustain. Environ.*, vol. 1, pp. 1-6, 2019.
30. J. E. Shigley and C. R. Michke, *Mechanical Engineering Design - 8th ed*., New York: McGraw Hill, 2008
31. B. P. Patel, H. R. Prajapati, and D. B. Thakar, “Critical Review on Design of Shaft with Multiple Discontinuities and Combined Loadings,” *Proc. Int. Conf. Contemp. Issue. Eng. Technol.*, pp. 7-14, 2014.
32. M. G. D. Marudachalam, K. Kanthavel, and R. Krishnaraj, “Optimization of Shaft Design under Fatigue Loading Using Goodman Method,” *Int. J. Sci. Eng. Res.*, vol. 2, pp. 1-5, 2011.
33. A. A. Adekunle, S. B. Adejuyigbe, and O. T. Arulogun, “Development of CAD Software for Shaft under Various Loading Conditions,” *Proc. Eng.*, vol. 38, pp. 1962-1983, 2012.
34. D. K. Padhal and D. B. Meshram, “Analysis and Failure Improvement of Shaft of Gear Motor in CRM Shop,” *Int. J. Eng. Sci.*, vol. 3, pp. 17-24, 2013.
35. S. G. Kolgiri, S. D. Martande, N. S. Motgi, and S. Nitin, “Stress Analysis for Rotor Shaft of Electric Motor,” *Int. J. App;. Innov. Eng. Manag.*, vol. 2, no. 7, pp. 136-141, 2013.
36. R. S. Khurmi and J. K. Gupta, *Text Book of Machine Design*, Kolkata: Eurasia Publishing House, 2005.